

Biocatalytic Reductions of Baylis–Hillman Adducts

Adam Z. Walton, W. Colin Conerly, Yuri Pompeu, Bradford Sullivan, and Jon D. Stewart*

Department of Chemistry, 126 Sisler Hall, University of Florida, Gainesville, Florida 32611, United States

Supporting Information

ABSTRACT: Baylis–Hillman adducts are highly useful synthetic intermediates; to enhance their value further, we sought enantioselective complementary alkene reductases to introduce chirality. Two solutions emerged: (1) a wild-type protein from *Pichia stipitis* (OYE 2.6), whose performance significantly outstrips that of the standard enzyme (*Saccharomyces pastorianus* OYE1), and (2) a series of OYE1 mutants at position 116 (Trp in the wild-type enzyme). To understand how mutations could lead to inverted enantioselectivity, we solved the X-ray crystal structure of the Trp116Ile OYE1 variant complexed with a cyclopentenone substrate. This revealed key protein–ligand interactions that control the orientation of substrate binding above the FMN cofactor.

KEYWORDS: old yellow enzyme, alkene reductase, enoate reductase, Baylis–Hillman, Roche's ester, X-ray crystallography, enantioselective



INTRODUCTION

The use of alkene reductases for stereoselective C=C bond reduction has become increasingly common.^{1–13} Although early library building and profiling efforts focused primarily on simple model compounds, recent attention has turned toward targets with more complex structures and correspondingly greater synthetic utility. In this regard, Baylis–Hillman adducts are particularly attractive substrates since their reductions provide chiral β -hydroxy ketones and esters from readily available starting materials.¹⁴ We therefore turned to our library of cloned alkene reductases for solutions. When these proved insufficient, except for *Pichia stipitis* OYE 2.6, we explored a more general strategy combining protein engineering and X-ray crystallography whose first fruits are reported here.

RESULTS AND DISCUSSION

We chose three representative Baylis–Hillman adducts whose reduction products are useful chiral synthons (Table 1). Reduction of methyl 2-(hydroxymethyl)acrylate **1** yields Roche's ester, which has been used to prepare a variety of commercially valuable natural products (recently summarized in ref 14). Chiral hydroxymethylcycloketones derived from 2-(hydroxymethyl)-2-cyclohexenone **2** and 2-(hydroxymethyl)-2-cyclopentenone **3** can be used directly for synthesis or oxidized to the corresponding lactones (see refs 15, 16 and references therein). After synthesis by literature methods,^{17–19} each alkene was tested as a substrate for our collection of purified alkene reductases²⁰ in the presence of an NADPH regeneration system (glucose/glucose dehydrogenase). *Saccharomyces pastorianus* OYE1, the prototypical flavoprotein alkene reductase, showed very high *R* stereoselectivity toward **1** but poor conversion efficiency (Table 1). The same enzyme was unable to reduce cyclohexenone **2**. This was unexpected since

S. pastorianus OYE1 converted the nearly isosteric 2-ethylcyclohexenone to the corresponding *S* product with 94% ee.¹ Finally, although *S. pastorianus* OYE1 partially reduced cyclopentenone **3** (51% conversion), the corresponding *R* product was isolated with only 60% ee. Similar or worse results were observed for nearly all of the wild-type enzymes in our cloned alkene reductase collection (see Supporting Information).

The only positive exception was provided by wild-type *Pichia stipitis* OYE 2.6, which completely reduced **1**, **2**, and **3** with good to excellent stereoselectivities (Table 1). We originally cloned and overexpressed this enzyme because it contained Ile at the position corresponding to Trp 116 of *S. pastorianus* OYE1.²¹ Despite sharing 42.7% sequence identity with *S. pastorianus* OYE1, *P. stipitis* OYE 2.6 has consistently demonstrated superior properties, including complementary stereoselectivity in some cases.²²

Although OYE 2.6 largely solved the problem of *S*-selective reductions of **1**–**3**, we also explored the possibility that *S. pastorianus* OYE1 variants might provide complementary performance. Our earlier studies showed that amino acid replacements at position 116 led to significantly altered stereoselectivities;²¹ we therefore created and screened a systematic library of Trp 116 replacements for reductions of alkenes **1**, **2**, and **3** (Table 1). For the Roche's ester precursor **1**, we identified two OYE1 variants (W116H and W116Q) that afforded the *S* enantiomer with high stereoselectivity, nicely complementing the *R*-selective wild-type enzyme (>98% ee). Three other amino acids (Phe, Tyr, and Val) significantly increased the extent of conversion,

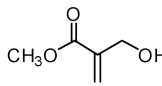
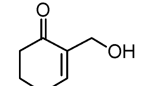
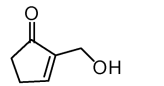
Special Issue: Biocatalysis and Biomimetic Catalysis for Sustainability

Received: April 30, 2011

Revised: June 14, 2011

Published: July 19, 2011

Table 1. Reductions of Baylis–Hillman Adducts by Alkene Reductases

| Protein | Substrate | | | | | |
|--|--|-------------------|---|-------------------|--|-------------------|
| |  1 | |  2 | |  3 | |
| | % conv | % ee ^a | % conv | % ee ^b | % conv | % ee ^c |
| <i>S. pastorianus</i> OYE1 mutants (116 residue) | | | | | | |
| Trp (wt) | 19 | >98 (R) | ≤5 | N.D. | 51 | 60 (R) |
| Ala | 9 | 90 (R) | 84 | >98 (S) | >98 | 72 (S) |
| Val | 52 | 86 (R) | 84 | >98 (S) | 97 | 92 (S) |
| Tyr | 68 | 76 (R) | >98 | >98 (S) | >98 | 87 (S) |
| Phe | 37 | 70 (R) | >98 | >98 (S) | 98 | >98 (S) |
| Ser | 13 | 46 (R) | 84 | >98 (S) | 87 | >98 (S) |
| Ile | 50 | 9 (R) | >98 | >98 (S) | >98 | 91 (S) |
| Arg | ≤5 | N.D. | ≤5 | N.D. | ≤5 | N.D. |
| Pro | ≤5 | N.D. | 14 | >98 (S) | 16 | 77 (S) |
| Thr | ≤5 | N.D. | 28 | >98 (S) | 44 | >98 (S) |
| Cys | ≤5 | N.D. | 31 | >98 (S) | 47 | 77 (S) |
| Lys | ≤5 | N.D. | 60 | >98 (S) | 75 | 76 (S) |
| Glu | ≤5 | N.D. | 93 | 90 (S) | 96 | 88 (S) |
| Asp | ≤5 | N.D. | >98 | 91 (S) | 95 | 77 (S) |
| Gly | 14 | 16 (S) | 98 | >98 (S) | >98 | 86 (S) |
| Leu | >98 | 20 (S) | >98 | >98 (S) | >98 | 57 (S) |
| Asn | >98 | 41 (S) | >98 | >98 (S) | >98 | 89 (S) |
| Met | 15 | 64 (S) | >98 | >98 (S) | >98 | 86 (S) |
| His | 67 | 97 (S) | >98 | >98 (S) | >98 | 77 (S) |
| Gln | 78 | >98 (S) | >98 | >98 (S) | >98 | 89 (S) |
| <i>P. stipitis</i> OYE 2.6 | >98 | >98 (S) | >98 | >99 (S) | >98 | 76 (S) |

^a Absolute configurations were assigned by retention time comparison to an authentic sample of the *R* reduction product (Sigma). ^b Absolute configurations were assigned by retention time comparisons to an authentic sample of *S* reduction product prepared according to ref 15. ^c Absolute configurations were assigned by retention time comparisons to an authentic sample of *S* reduction product.

although the *R* selectivity was somewhat diminished. This suggests that further protein engineering efforts may solve both the conversion and stereoselectivity issues simultaneously. Although cyclohexenone **2** is not a substrate for wild-type OYE1, we identified variants that yielded the *S* product in >98% ee and with complete conversion and two others with only slightly poorer properties (Table 1). For cyclopentenone **3** (a relatively poor substrate for wild-type *S. pastorianus* OYE1), many Trp 116 substitutions favored the *S* product, and one (Phe) afforded both complete conversion and >98% ee (Table 1). Interestingly, this performance was even better than the wild-type *P. stipitis* OYE 2.6.

OYE1 catalyzes hydride transfer from reduced flavin mononucleotide (FMN) to the electron-deficient β -carbon of the substrate along with proton transfer from an opposing general acid (likely the side chain of Tyr 196²³) to yield net trans addition of H₂.²⁴ Thus, the stereochemical outcome depends upon which face of the alkene π -system faces the FMN, suggesting that substrate **3** binds in opposite orientations to the wild-type OYE1

and the W116I mutant. We tested this hypothesis by crystallizing the W116I mutant of OYE1, then soaking the crystals in storage buffer containing 10 mM enone **3**. The soaked crystals diffracted to 1.7–1.4 Å, and the structure was solved by molecular replacement using the wild-type OYE1 structure as a search model.²⁵ The electron density maps at 1.4 Å resolution were very clear, which allowed for efficient model building (Figure 1). As anticipated, the overall structure of the W116I mutant was nearly identical to that of wild type enzyme. Inspecting the difference electron density map ($mF_o - DF_c$) allowed regions of poor fit to be rebuilt, and this process was continued iteratively until error statistics converged ($R_{\text{free}} = 0.17$, $R_{\text{work}} = 0.15$). A region of electron density located above the isoalloxazine ring of the FMN corresponded to the bound substrate. The final model coordinates have been deposited into the PDB under code 3RND.

Substrate **3** bound with high occupancy (~80%), and we systematically explored potential fits of its structure within the observed electron density. An attempt to use a single binding

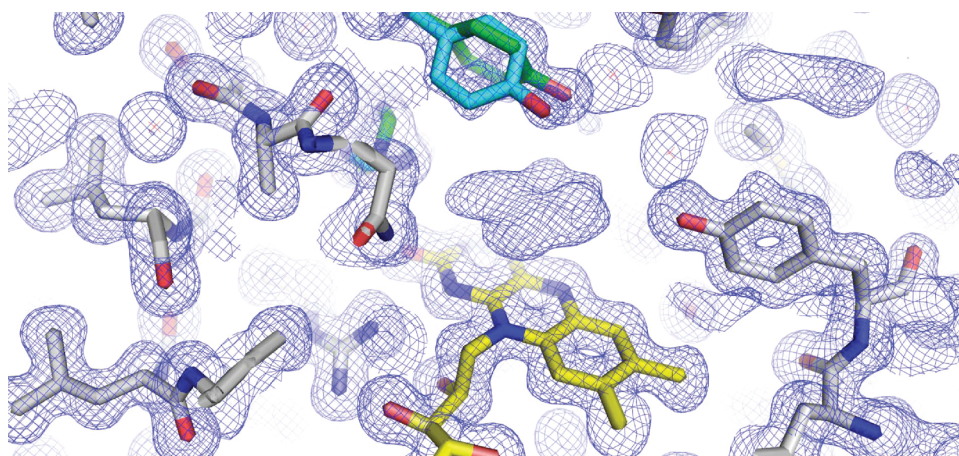


Figure 1. Electron density map in the active site region. $2mF_0 - DF_c$ electron density is displayed at the 0.5σ contour level along with the final model for the protein. Atoms are displayed in CPK standard colors except for FMN (carbons colored yellow) and side chains of His191 and Tyr 196 (carbons colored light blue or green). Two different side-chain orientations were observed for these residues within the crystal, likely because of two different substrate binding orientations. The area of electron density between the FMN and Tyr 196 corresponds to bound enone 3.

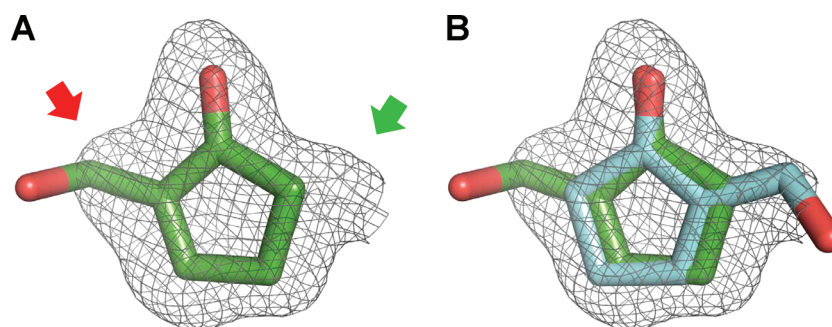


Figure 2. Location of cyclopentenone 3 within the observed electron density (0.4σ contour level). A. Attempted fit by a single ligand orientation. Red and green arrows indicate regions of negative and positive electron density peaks, respectively, in the difference map (not shown). B. Successful fit by two ligand populations. Carbons in binding mode 1 are shown in green, and those in binding mode 2 are light blue. Note that the lack of electron density for the OH is likely due to facile C–O bond rotation. Figures were rendered with PyMOL.³¹

orientation for enone 3 yielded a region of surplus electron density on one side of the calculated map and a deficit of electron density on the other when compared with the observed map (Figure 2). We therefore modeled enone 3 as a 1:1 mixture of two different binding orientations. The difference map for this arrangement showed no significant features at the 3σ contour level, indicating that a mixture of ligand binding modes adequately accounted for all of the electron density data. Binding mode 1 positions the *re* face of the substrate for hydride transfer from FMN H_2 ; in binding mode 2, the opposite (*si*) face of the substrate is poised to accept a hydride. Diffraction data from three different soaked crystals were examined, and a mixture of binding orientations was observed in all three cases.

In both substrate binding orientations, the carbonyl oxygen lies between the side chains of Asn 194 and His 191 with distances of ~ 3 Å and the cyclopentene moiety of the ligand is oriented parallel to the isoalloxazine ring of FMN. The carbonyl oxygen location is consistent with hydrogen bonding interactions with residues known to participate in catalysis (Figure 3).²⁶ Similar hydrogen bonding has been observed between wild-type OYE1 and the hydroxyl moiety of the inhibitor *p*-hydroxybenzaldehyde.²⁵ The orientation of the hydroxymethyl side chain is the key difference between the two substrate binding modes.

Binding mode 1 places this moiety on the side opposite Ile 116. The hydroxyl oxygen appears to rotate freely and lies near a water molecule and the side chain of Asn 194. The other substrate binding mode places the hydroxymethyl group near the side chains of Ile 116 and Thr 37. One likely position for the hydroxyl moiety coincides with a region of electron density centered 2.87 Å from the side chain of Thr 37. Such a location would be consistent with a hydrogen bond; however, this would also place the substrate hydroxyl less than 2 Å from the phenolic oxygen of Tyr 196, where it would experience steric clash. The electron density map indicates a second orientation for the Tyr 196 side chain (Figure 1), and we believe that these correspond to the two substrate binding modes (Figure 3). Movement of Tyr 196 away from the substrate side chain would, in turn, cause steric clash with His 191, which is also found in two orientations according to the electron density map.

Several factors argue that binding mode 1 (which would lead to the minor *R* product) does not represent a favorable Michaelis complex for catalysis. The angle formed by FMN N_{10} – N_5 –substrate β -carbon is 78° . In his survey of flavoprotein crystal structures, Fraaije observed angles between 96° and 117° for productive binding modes leading to hydride transfer.²⁷ In addition, the likely position of Tyr 196 places its phenolic oxygen 4.45 Å

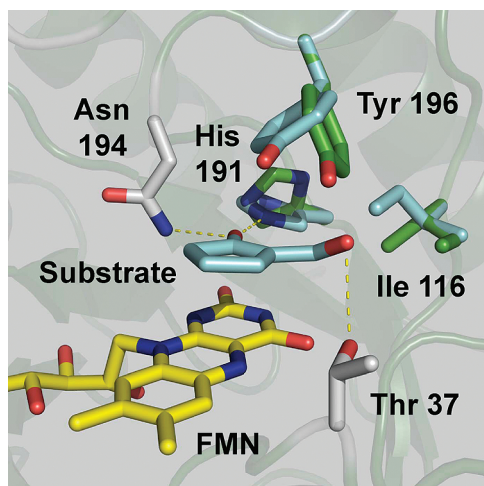


Figure 3. Enzyme–substrate complex for cyclopentenone **3** and W116I OYE1. Protein atoms are displayed in CPK standard colors except for FMN (carbons colored yellow) and the side chains of His 191 and Tyr 196 (carbons colored light blue or green). Only the catalytically favorable complex for enone **3** is shown (binding mode 2).

from the substrate α -carbon, too far for efficient proton transfer. Finally, placing the substrate's hydroxymethyl group opposite the side chain of Ile 116 makes it difficult to understand why replacing Trp 116 with Ile should be important in altering the enzyme's stereochemical preference.

By contrast, the substrate orientation in binding mode 2 (which would lead to the major *S* product) appears to be a productive complex and provides a clear rationale for the effect of replacing Trp 116 with Ile. The angle formed by FMN N₁₀–N₅–substrate β -carbon is 98° and the FMN N₅–substrate β -carbon distance is 3.54 Å; both values are within the “normal” ranges for hydride transfer. The distance from the phenolic oxygen in the allowed conformation of Tyr196 to the substrate C $_{\alpha}$ is 2.98 Å. Finally, the close proximity of the substrate hydroxymethyl group to the side chain of the residue at position 116 suggests that relieving steric congestion by replacing a bulky indole with an isobutyl group would allow the enone to enter the active site in binding mode 2. Net trans addition of H₂ would afford the *S* product, as observed.

CONCLUSIONS

Taken together, these results demonstrate two potential solutions to the “other enantiomer” problem for alkene reductases. Whereas most wild-type enzymes had properties inferior to those of *S. pastorianus* OYE1, *P. stipitis* OYE 2.6 was an important exception. We are continuing to explore the properties of this highly interesting biocatalyst that often complement those of OYE1.²² One key difference between OYE 2.6 and OYE1 lies in a loop²⁸ that closely approaches the substrate binding site in the latter. In OYE 2.6, this region lacks two amino acids, which may lead to a more open and accommodating active site. This effect can be seen in the crystal structures of *Bacillus subtilis* YqjM²⁹ and *Enterobacter cloacae* PETN reductase.³⁰

In cases that neither wild-type OYE1 nor OYE 2.6 provide an acceptable catalyst for a desired reaction, site saturation mutagenesis of Trp 116 is a simple strategy that can yield significant improvements. If these first-generation improvements prove insufficient, they can be used as the starting point for a larger

program of protein engineering.¹¹ Directly observing the alterations in enzyme–substrate interactions by X-ray crystallography provides extremely valuable guidance in understanding the effects of mutations and also in suggesting avenues for further improvement. Here, we uncovered evidence for multiple substrate binding modes, only one of which favored catalysis. It is possible that further changes will eliminate the formation of the unproductive complex, which should maximize catalytic rates.

ASSOCIATED CONTENT

S Supporting Information. Experimental procedures for creating, isolating, and screening the collection of Trp 116 replacements for *S. pastorianus* OYE1; details for substrate synthesis; details for X-ray structure determination. This material is available free of charge via the Internet at <http://pubs.acs.org>.

AUTHOR INFORMATION

Corresponding Author

*Phone/Fax: 352.846.0743. E-mail: jds2@chem.ufl.edu.

ACKNOWLEDGMENT

Financial support by the National Science Foundation (CHE-0615776 and CHE-1111791) and the U.S. Army Advanced Civilian Schooling Program is gratefully acknowledged. We also thank Professor Steven Bruner for his guidance in crystallography studies, Professor Robert McKenna and the U.F. Center for Structural Biology for diffractometer access and many helpful discussions, and Dr. Annie Héroux (Macromolecular Crystallography Research Resource (PXRR), Brookhaven National Laboratory) for synchrotron data collection.

REFERENCES

- (1) Swiderska, M. A.; Stewart, J. D. *J. Mol. Catal. B: Enzym.* **2006**, *42*, 52–54.
- (2) Chaparro-Riggers, J. F.; Rogers, T. A.; Vazquez-Figueroa, E.; Polizzi, K. M.; Bommaris, A. S. *Adv. Synth. Catal.* **2007**, *349*, 1521–1531.
- (3) Hall, M.; Stueckler, C.; Kroutil, W.; Macheroux, P.; Faber, K. *Angew. Chem., Int. Ed.* **2007**, *46*, 3934–3937.
- (4) Stueckler, C.; Hall, M.; Ehammer, H.; Pointner, E.; Kroutil, W.; Macheroux, P.; Faber, K. *Org. Lett.* **2007**, *9*, 5409–5411.
- (5) Stuermer, R.; Hauer, B.; Hall, M.; Faber, K. *Curr. Opin. Chem. Biol.* **2007**, *11*, 203–213.
- (6) Hall, M.; Stueckler, C.; Ehammer, H.; Pointner, E.; Oberdorfer, G.; Gruber, K.; Hauer, B.; Stuermer, R.; Kroutil, W.; Macheroux, P.; Faber, K. *Adv. Synth. Catal.* **2008**, *350*, 411–418.
- (7) Hall, M.; Stueckler, C.; Hauer, B.; Stuermer, R.; Friedrich, T.; Breuer, M.; Kroutil, W.; Faber, K. *Eur. J. Org. Chem.* **2008**, 1511–1516.
- (8) Kosjek, B.; Fleitz, F. J.; Dormer, P. G.; Kuethe, J. T.; Devine, P. N. *Tetrahedron: Asymmetry* **2008**, *19*, 1403–1406.
- (9) Schweiger, P.; Gross, H.; Wesener, S.; Deppenmeier, U. *Appl. Microbiol. Biotechnol.* **2008**, *80*, 995–1006.
- (10) Adalbjörnsson, B. V.; Toogood, H.; Fryszkowska, A.; Pudney, C. R.; Jowitt, T. A.; Leys, D.; Scrutton, N. S. *ChemBioChem* **2009**, *11*, 197–207.
- (11) Bougioukou, D. J.; Kille, S.; Taglieber, A.; Reetz, M. T. *Adv. Synth. Catal.* **2009**, *351*, 3287–3305.
- (12) Burda, E.; Krausser, M.; Fischer, G.; Hummel, W.; Müller-Uri, F.; Kreis, W.; Gröger, H. *Adv. Synth. Catal.* **2009**, *351*, 2787–2790.
- (13) Hirata, T.; Matsushima, A.; Sato, Y.; Iwasaki, T.; Nomura, H.; Watanabe, T.; Toyoda, S.; Izumi, S. *J. Mol. Catal. B: Enzym.* **2009**, *59*, 158–162.

- (14) Stueckler, C.; Winkler, C. K.; Bonnekessel, M.; Faber, K. *Adv. Synth. Catal.* **2010**, *352*, 2663–2666.
- (15) Chen, A.; Xu, J.; Chiang, W.; Chai, C. L. L. *Tetrahedron* **2010**, *66*, 1489–1495.
- (16) Mase, N.; Inoue, A.; Nishio, M.; Takabe, K. *Bioorg. Med. Chem. Lett.* **2009**, *19*, 3955–3958.
- (17) Yu, C. Z.; Liu, B.; Hu, L. Q. *J. Org. Chem.* **2001**, *66*, 5413–5418.
- (18) Rezgui, F.; El Gaied, M. M. *Tetrahedron Lett.* **1998**, *39*, 5965–5966.
- (19) Kar, A.; Argade, N. P. *Synthesis* **2005**, 1234–1236.
- (20) Bougioukou, D. J. Ph.D. Thesis, University of Florida, Gainesville, FL, 2006.
- (21) Padhi, S. K.; Bougioukou, D. J.; Stewart, J. D. *J. Am. Chem. Soc.* **2009**, *131*, 3271–3280.
- (22) Bougioukou, D. J.; Walton, A. Z.; Stewart, J. D. *Chem. Commun.* **2010**, *46*, 8558–8560.
- (23) Kohli, R. M.; Massey, V. *J. Biol. Chem.* **1998**, *273*, 32763–32770.
- (24) Karplus, P. A.; Fox, K. M.; Massey, V. *FASEB J.* **1995**, *9*, 1518–1526.
- (25) Fox, K. M.; Karplus, P. A. *Structure* **1994**, *2*, 1089–1105.
- (26) Brown, B. J.; Deng, Z.; Karplus, P. A.; Massey, V. *J. Biol. Chem.* **1998**, *273*, 32753–32762.
- (27) Fraaije, M. W.; Mattevi, A. *Trends Biochem. Sci.* **2000**, *25*, 126–132.
- (28) Residues 293–302, OYE1 numbering.
- (29) Fitzpatrick, T. B.; Amrhein, N.; Macheroux, P. *J. Biol. Chem.* **2003**, *278*, 19891–19897.
- (30) Toogood, H.; Fryszkowska, A.; Hulley, M.; Sakuma, M.; Mansell, D.; Stephens, G. M.; Gardiner, J. M.; Scrutton, N. S. *ChemBioChem* **2011**, *12*, 738–749.
- (31) DeLano, W. L. *The PyMOL Molecular Graphics System*, 2002 (<http://www.pymol.org>).